The Journal of Infectious Diseases

MAJOR ARTICLE

Varicella-Zoster Virus Infection of Primary Human Spinal Astrocytes Produces Intracellular Amylin, Amyloid-β, and an Amyloidogenic Extracellular Environment

Andrew N. Bubak,[1] Christina N. Como,[1] Christina M. Coughlan,[1,2,3] Noah R. Johnson,[1,2,3] James E. Hassell Jr,[1] Teresa Mescher,[1] Christy S. Niemeyer,[1] Ravi Mahalingam,[1] Randall J. Cohrs,[1,4] Timothy D. Boyd,[1,2,3] Huntington Potter,[1,2,3] Holger A. Russ,[5] and Maria A. Nagel[1,6]

[1]Department of Neurology, University of Colorado School of Medicine, Aurora, Colorado, USA, [2]Rocky Mountain Alzheimer's Disease Center, University of Colorado School of Medicine, Aurora, Colorado, USA, [3]Linda Crnic Institute for Down Syndrome Research, University of Colorado School of Medicine, Aurora, Colorado, USA, [4]Department of Immunology and Microbiology, University of Colorado School of Medicine, Aurora, Colorado, USA, [5]Barbara Davis Center for Diabetes, University of Colorado School of Medicine, Aurora, Colorado, USA, and [6]Department of Ophthalmology, University of Colorado School of Medicine, Aurora, Colorado, USA

Background. Herpes zoster is linked to amyloid-associated diseases, including dementia, macular degeneration, and diabetes mellitus, in epidemiological studies. Thus, we examined whether varicella-zoster virus (VZV)-infected cells produce amyloid.

Methods. Production of intracellular amyloidogenic proteins (amylin, amyloid precursor protein [APP], and amyloid-β [Aβ]) and amyloid, as well as extracellular amylin, Aβ, and amyloid, was compared between mock- and VZV-infected quiescent primary human spinal astrocytes (qHA-sps). The ability of supernatant from infected cells to induce amylin or Aβ42 aggregation was quantitated. Finally, the amyloidogenic activity of viral peptides was examined.

Results. VZV-infected qHA-sps, but not mock-infected qHA-sps, contained intracellular amylin, APP, and/or Aβ, and amyloid. No differences in extracellular amylin, Aβ40, or Aβ42 were detected, yet only supernatant from VZV-infected cells induced amylin aggregation and, to a lesser extent, Aβ42 aggregation into amyloid fibrils. VZV glycoprotein B (gB) peptides assembled into fibrils and catalyzed amylin and Aβ42 aggregation.

Conclusions. VZV-infected qHA-sps produced intracellular amyloid and their extracellular environment promoted aggregation of cellular peptides into amyloid fibrils that may be due, in part, to VZV gB peptides. These findings suggest that together with host and other environmental factors, VZV infection may increase the toxic amyloid burden and contribute to amyloid-associated disease progression.

Keywords. varicella-zoster virus; amyloid; amylin; Aβ42; Alzheimer disease; astrocytes.

Varicella-zoster virus (VZV) is latent in ganglionic neurons in >90% of the world population [1–3]. With aging and immunosuppression, VZV reactivates and travels transaxonally to multiple organs, typically producing zoster (shingles), as well as multisystem disease including stroke, keratitis, retinal necrosis, myelopathy, and gastritis with or without rash [4, 5]. Recent studies have linked zoster with 3 diseases characterized by amyloid deposition: dementia, neovascular age-related macular degeneration (AMD), and diabetes mellitus (DM). In a retrospective cohort study of healthy and herpes zoster ophthalmicus subjects, herpes zoster ophthalmicus conferred a 2.97-fold greater risk of developing dementia, of which Alzheimer disease (AD) was most common, over a 5-year period ($P < .001$) [6]; this risk was still increased, but to a lesser degree, if zoster occurred in any dermatome (1.11-fold; $P < .0014$) and antiviral therapy reduced the risk [7]. Zoster also conferred a 4.62-fold increased risk of developing neovascular AMD over 3 years ($P < .001$) [8] and a deterioration in glycemic control among subjects with DM [9].

Although these previous studies show an epidemiological association between VZV reactivation (zoster) and 3 amyloid-associated diseases, the direct role of VZV infection in amyloid production has not been demonstrated. During reactivation from sensory ganglia, VZV can enter the central nervous system along neurites that synapse within the spinal cord. Because VZV preferentially infects spinal astrocytes [10, 11], we determined whether VZV infection of primary human spinal astrocytes (HA-sps) produced increased levels of amyloid and amyloidogenic cellular peptides, including amyloid-β (Aβ) found in AD plaques and in drusen of AMD, as well as amylin found in AD plaques and pancreatic amyloid deposits in DM. Furthermore, we examined predicted amyloidogenic viral peptides within VZV glycoprotein B (gB) to determine whether they may contribute to VZV's ability to accelerate amyloid deposition.

Received 29 August 2019; editorial decision 21 October 2019; accepted 23 October 2019; published online October 29, 2019.

Correspondence: M. A. Nagel, MD, Department of Neurology, University of Colorado School of Medicine, 12700 E. 19th Avenue, Mail Stop B182, Aurora, CO 80045, USA (maria.nagel@cuanschutz.edu).

The Journal of Infectious Diseases® 2020;221:1088–97

DOI: 10.1093/infdis/jiz560

METHODS

Cells and Virus

Quiescent primary HA-sps (qHA-sps; Sciencell) were cocultured with either VZV-infected HA-sps (40 plaque-forming units/cm^2; VZV Gilden strain, GenBank No. MH379685) or uninfected HA-sps (mock infected) as described [11]. Cells and supernatants (spun at 2000 RPM for 5 minutes to eliminate nonadherent VZV-infected cells [11]) were analyzed at 3 days postinfection (DPI; height of cytopathic effect).

Reverse Transcription and Quantitative PCR

RNA was extracted and reverse transcribed as described [11]; cDNA was analyzed by quantitative polymerase chain reaction (qPCR) using primers for amylin (Life Technologies; Hs00169095_m1), amyloid precursor protein (APP; Integrated DNA Technologies; NM_201414), VZV (FWD: CGAACACGTTCCCCATCAA; REV: CCCGGCTTTGTTAGTTTTGG; probe: FAM/TCCAGGTTTTAGTTGATACCA-/BkFQ/), and glyceraldehyde-3-phosphate-dehydrogenase (GAPDH; FWD: CACATGGCCTCCAAGGAGTAA; REV: TGAGGGTCTCTCTCTTCCTCTTGT; probe: VIC/CTGGACCACCAGCCCCAGCAAG-/BkFQ/) as described [12]. Data were normalized to GAPDH and analyzed using the ΔΔ cycle threshold (Ct) method or ΔCt method when only the VZV-infected group had detectable transcripts.

Immunofluorescence Antibody Assay and Intracellular Thioflavin-T Fluorescence Assay

Quiescent HA-sps were plated in clear-bottom plates (24-well μ-plate; ibidi) and infected. At 3 DPI, cells were washed with phosphate-buffered saline, fixed for 20 minutes in 4% paraformaldehyde, permeabilized with 0.1% Triton-X for 10 minutes, and blocked in 5% normal goat serum. To determine VZV colocalization with amylin and amyloid or with Aβ and amyloid, 2 sets of immunofluorescence antibody assays (IFAs) were performed as described [11]. In the first set, mock- and VZV-infected qHA-sps were incubated with primary mouse anti-VZV gB (1:250 dilution; Abcam) and rabbit antiamylin antibodies (1:500; Abcam). In the second set, cells were incubated with primary rabbit anti-VZV 63 (1:10 000) [13] and mouse antiamyloid-β aa1–16 antibodies (1:500; BioLegend). Secondary antibodies were Alexa Fluor 647 goat anti-mouse and Alexa Fluor 594 goat anti-rabbit IgGs (both at 1:500; Life Technologies). Nuclei were stained with 2 μg/mL 4′,6-diamidino-2-phenylindole (DAPI; Vector Labs). To detect amyloid-like fibrillar structures comprised of amylin, Aβ, and/or other amyloidogenic peptides, both sets were then incubated for 8 minutes at room temperature with filtered 1% thioflavin-T (Thio-T) in distilled water (MilliporeSigma), dehydrated in 75%, 80%, and 95% ethanol for 3 minutes each, and rehydrated in deionized water. Wells were imaged using an Olympus IX73 fluorescence microscope with cellSens imaging software (Olympus Corporation).

Acyclovir Treatment

HA-sps were plated on clear-bottom plates for IFA and in 24-well plates for DNA analysis then mock and VZV infected. After 24 hours, 44 μM of acyclovir (MilliporeSigma) or vehicle dimethyl sulfoxide (DMSO) was added and replenished every 24 hours. At 1, 2, and 3 DPI, DNA was extracted and qPCR using primers for GAPDH and VZV was performed [11]; at 1 and 3 DPI, IFA analysis and a Thio-T assay as above was performed.

Amylin and Aβ ELISA

Mock- and VZV-infected cell supernatants were analyzed in duplicate for amylin by an enzyme-linked immunosorbent assay (ELISA; MilliporeSigma). Similarly, the processed forms of APP (Aβ38, Aβ40, and Aβ42) were quantified using the V-Plex Plus Aβ peptide panel 1 ELISA (Mesoscale Discovery).

Peptides and Thio-T Fluorescence Assay

VZV gB was scanned for predicted amyloidogenic regions (waltz.switchlab.org). Based on 5 regions identified, peptides spanning 3 selected amyloidogenic regions of interest (ROI 1, 2, and 3) and spanning a nonamyloidogenic region (NEG) were synthesized (GenScript Biotech Corp). Lyophilized peptides were resuspended in 50 μL DMSO then diluted in nanopure water (final concentration, 2 mg/mL). Human amylin was resuspended in nanopure water (final concentration, 156 μM). For aggregation assays, 10, 50, and 100 μg of each VZV peptide was further diluted in 200 μL of nanopure water with or without 50 μM amylin (within the estimated physiological range [14]), or 4 μM Aβ42 (optimized concentration for Thio-T and aggregation assays), and then incubated at 37°C for 24 hours or 1 hour, respectively. Five microliters of peptide solution was added to 195 μL of nanopure water and 75 μL of 13.5 μM Thio-T (in 50 mM glycine) in a black 96-well plate, incubated in the dark for 10 minutes, and analyzed on a fluorescence plate reader. Excitation and emission wavelengths were 440 and 490 nm, respectively. Final concentrations for each VZV peptide solution were approximately 3, 15, and 30 μM. In a similar experiment, a low (5 μM) or high (50 μM) concentration of amylin was added to a constant 15 μM ROI 3 solution. All samples were run in triplicate.

Transmission Electron Microscopy

Mock- or VZV-infected cell supernatants were incubated with 50 μM human amylin at 37°C for 72 hours or with 4 μM Aβ42 for 1 hour. A negative charge was applied to copper mesh grids coated with formvar and carbon using the PELCO easiGlow Discharge system. For each sample, 5 μL was applied to a charged grid for 20 seconds and blotted with Whatman filter paper. Grids were rinsed with MilliQ water, stained with 0.75% uranyl formate, rinsed with water, air dried, and imaged on

a FEI Tecnai G2 Biotwin transmission electron microscope (TEM; FEI Company) at 80 kV with an Advanced Microscopy Techniques side-mount digital camera.

Statistical Analysis

A 1-way ANOVA corrected for multiple comparisons was used to test for differences in Thio-T fluorescence intensities of the ROI and NEG peptides at 3, 15, and 30 μM alone, as well as in the presence of amylin or Aβ42. Individual *t* tests corrected for multiple comparisons were used to test for statistical significance between amylin alone versus amylin/ROI 3 at both the low and high concentrations. α was set at .05.

RESULTS

VZV-Infected qHA-sps Contain Amylin, APP/Aβ Peptides, and Amyloid

To determine if VZV alters amylin and APP transcripts, mock- and VZV-infected qHA-sp RNA was analyzed by reverse transcription and qPCR at 3 DPI. Amylin transcripts were absent in mock-infected but present in VZV-infected qHA-sps (mean ΔCt ± SEM, 14.75 ± 0.67; n = 4). No differences in APP transcripts were seen.

Mock- and VZV-infected cells were analyzed by IFA using antibodies against: (1) VZV gB or VZV 63, (2) amylin, and (3) Aβ aa1–16, which detects both full-length APP and its processed forms (Aβ peptides), as well as by Thio-T fluorescence assay that detects β-sheets in amyloid-like fibrillar structures (prefibrillar oligomers and fibrils, referred to as amyloid hereafter). Mock-infected qHA-sps did not express VZV, amylin, or APP/Aβ and were Thio-T negative (Figure 1A and 1B, top rows). VZV-infected qHA-sps expressed VZV gB/63, amylin, and APP/Aβ and were Thio-T positive (Figure 1A and 1B, bottom rows; arrows indicate representative cells); amyloidogenic proteins and amyloid were not seen in uninfected bystander cells. Overall, VZV infection of qHA-sps induced amyloidogenic protein expression and amyloid.

VZV gB and Amyloid Persist After Acyclovir Treatment

To determine if ongoing VZV DNA replication is required for VZV gB expression and accumulation of amyloid, HA-sps were VZV infected then treated with vehicle or acyclovir at 1 DPI. PCR showed VZV DNA increasing in vehicle-treated cells over 3 days, whereas acyclovir significantly reduced levels of VZV

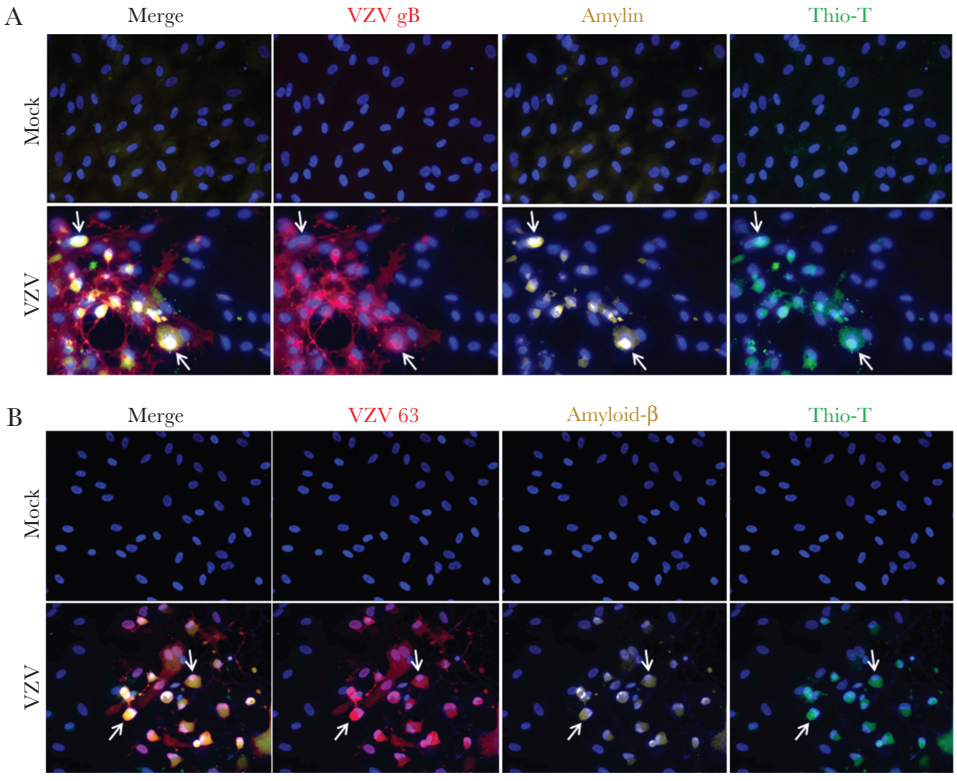

Figure 1. Varicella-zoster virus (VZV)-infected quiescent primary human spinal astrocytes (qHA-sps) contain amylin, amyloid precursor protein (APP)/amyloid-β (Aβ), and amyloid. Mock- and VZV-infected qHA-sps were analyzed at 3 days postinfection by an immunofluorescence antibody assay using antibodies against VZV glycoprotein B (gB) or open reading frame 63, amylin, and amyloid-β aa1–16 that detects full-length APP and its processed forms (Aβ peptides), as well as by a thioflavin-T (Thio-T) fluorescence assay that detects β-sheets in amyloid-like fibrillar structures (prefibrillar oligomers and fibrils). *A,* Mock-infected qHA-sps did not contain VZV gB or amylin and were Thio-T negative. VZV-infected qHA-sps contained VZV gB (red) and amylin (yellow) and were Thio-T positive (green; arrows indicate representative cells). Uninfected bystander cells in VZV cultures did not contain amylin and were Thio-T negative. *B,* Mock-infected qHA-sps did not contain VZV 63 or APP/Aβ and were Thio-T negative. VZV-infected cells contained VZV 63 (red) and APP/Aβ (yellow) and were Thio-T positive (green; arrows indicate representative cells). Uninfected bystander cells in VZV cultures did not contain APP/Aβ and were Thio-T negative. Blue corresponds to DAPI staining of cell nuclei (original magnification ×400).

DNA at 2 and 3 DPI (Figure 2A). At 1 DPI in both cultures, VZV gB-positive cells had no to minimal expression of amylin or APP/Aβ (Figure 2B and 2C, respectively) and were Thio-T negative. However, at 3 DPI, amylin and APP/Aβ were found in VZV gB-positive cells, albeit with fewer infected cells in the acyclovir-treated cultures (Figure 3A and 3B; arrows indicate representative cells; field taken of acyclovir-treated cultures had most concentrated areas of infection).

VZV-Infected qHA-sps Produce an Amyloidogenic Extracellular Environment Independent of Secreted Amylin, Aβ40, or Aβ42 Concentrations

Mock- and VZV-infected cell supernatants did not contain detectable amylin or Aβ38. No significant differences in Aβ40 or Aβ42 were detected between mock- and VZV-infected qHA-sps (Aβ40, mean ± SEM, 58.99 pg/mL ± 9.9 vs 23.99 pg/mL ± 10.34; Aβ42, mean ± SEM, 1.89 pg/mL ± 0.36 vs 1.20 pg/mL ± 0.41, respectively; $P > .05$, n = 2 and 3, respectively).

Although extracellular amyloidogenic peptides were not altered, we tested whether supernatants differed in their ability to induce cellular peptide aggregation by adding amylin or Aβ42. After adding amylin, mock-infected cell supernatant revealed minimal amyloid fibrils, whereas VZV-infected cell supernatant showed abundant fibrils (Figure 4A, arrows). After adding Aβ42, mock-infected cell supernatant revealed globular aggregates that differed from the branching amyloid structures seen in VZV-infected cell supernatant (Figure 4B, arrows). Thus, VZV-infected cell supernatant contained factors that promoted aggregation of amylin into amyloid fibrils and, to a lesser extent, of Aβ42 into more branched amyloid-like structures that were not induced by mock-infected cell supernatant.

VZV gB Contains Amyloidogenic Sequences

The ability of supernatant from VZV-infected qHA-sps to induce amyloid formation without increased amylin or Aβ levels raised the possibility that a viral peptide may contribute to amyloid formation. We focused on the transmembrane protein VZV gB because it is highly abundant during infection and represents the predominant antibody response in elderly subjects' sera [15]. The Waltz algorithm predicted 5 amyloidogenic sequences within VZV gB (GenBank, ABW06910.1). Of these, we selected 3 amyloidogenic regions of interest (ROI 1–3) and 1 region predicted to be NEG to synthesize and investigate (Figure 5A and 5B).

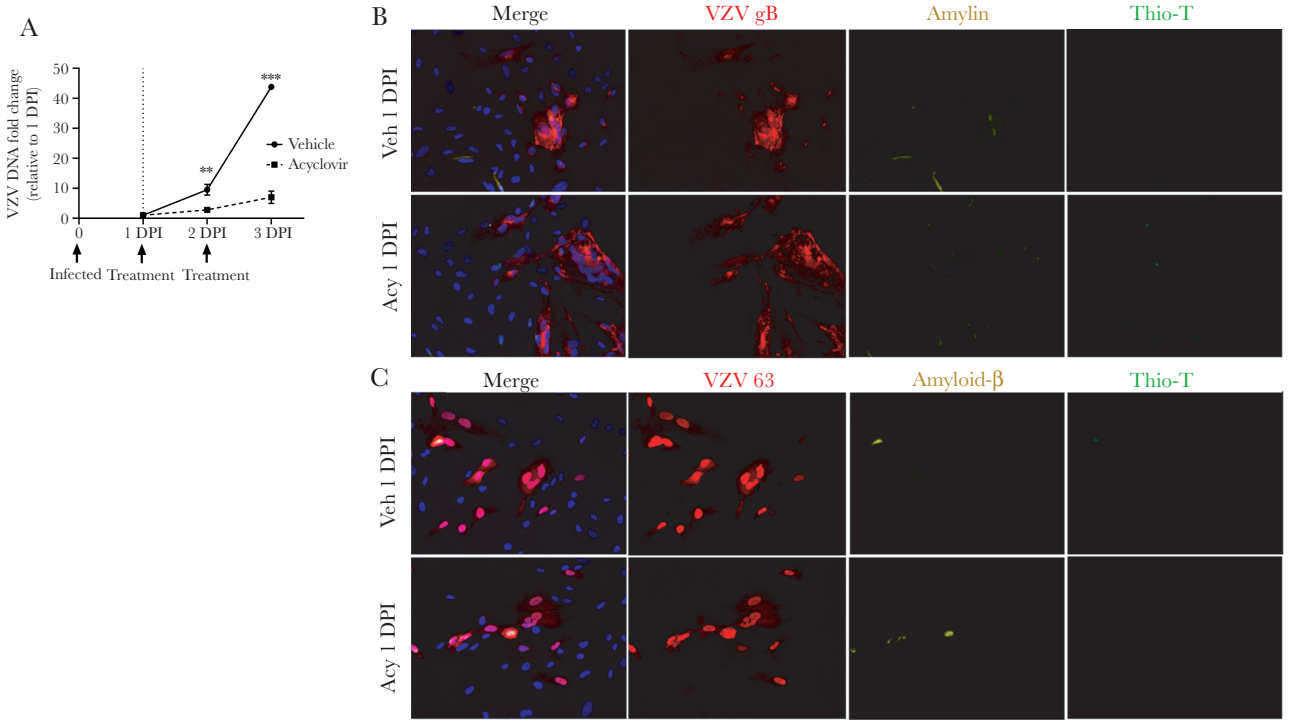

Figure 2. Acyclovir decreases varicella-zoster virus (VZV) DNA accumulation and no amyloid is detected early in infection. *A*, Primary human spinal astrocytes (HA-sps) were VZV infected then treated with either acyclovir or vehicle at 1 and 2 days postinfection (DPI). The VZV DNA fold change at 2 and 3 DPI, relative to the sample's corresponding 1 DPI, was compared between vehicle- and acyclovir-treated HA-sps. At 2 and 3 DPI, the VZV DNA fold changes in acyclovir-treated cells were significantly lower than in vehicle-treated cells. $^{**}P < .01$, $^{***}P < .001$; n = 3 independent experiments. *B*, Vehicle- and acyclovir-treated HA-sps were analyzed at 1 DPI by an immunofluorescence antibody assay using antibodies against VZV glycoprotein B (gB) or open reading frame 63, amylin, and amyloid-β (Aβ) aa1–16 that detects full-length amyloid precursor protein (APP) and its processed forms (Aβ peptides), as well as by a thioflavin-T (Thio-T) fluorescence assay that detects β-sheets in amyloid-like fibrillar structures (prefibrillar oligomers and fibrils). At 1 DPI, both vehicle- and acyclovir-treated, VZV-infected HA-sps contained VZV gB (red), no to minimal amylin (yellow), and were Thio-T negative. *C*, Similarly, both treatment groups expressed VZV 63 (red), minimal amyloid-β (yellow), and were Thio-T negative. Blue corresponds to DAPI staining of cell nuclei (original magnification ×400). Abbreviations: Acy, acyclovir; Veh, vehicle.

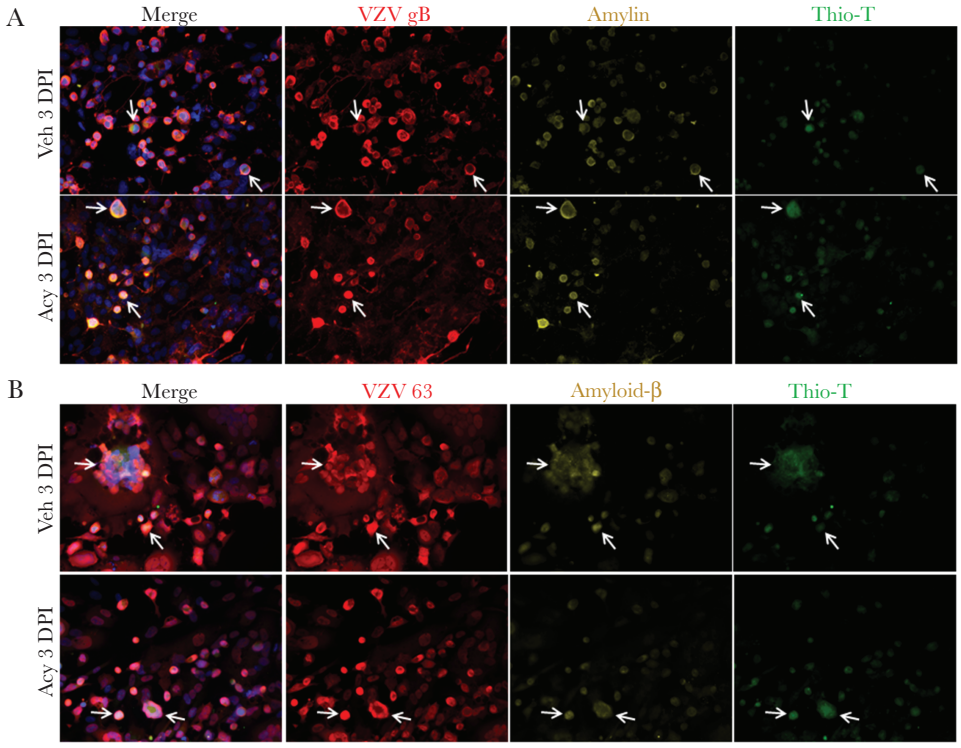

Figure 3. Acyclovir does not prevent the accumulation of amylin, amyloid-β, or amyloid at 3 days postinfection (DPI) in varicella-zoster virus (VZV)-infected primary human spinal astrocytes (HA-sps). *A*, Vehicle- and acyclovir-treated HA-sps were analyzed at 3 DPI by an immunofluorescence antibody assay using antibodies against VZV glycoprotein B (gB) or open reading frame 63, amylin, and amyloid-β (Aβ) aa1–16 that detects full-length amyloid precursor protein (APP) and its processed forms (Aβ peptides), as well as by a thioflavin-T (Thio-T) fluorescence assay that detects β-sheets in amyloid-like fibrillar structures (prefibrillar oligomers and fibrils). At 3 DPI, both vehicle- and acyclovir-treated, VZV-infected HA-sps contained VZV gB, amylin, and were Thio-T positive. *B*, Similarly, both treatment groups expressed robust VZV 63, amyloid-β, and were Thio-T positive. Arrows indicate representative cells containing VZV, amyloidogenic peptides, and amyloid. Blue corresponds to DAPI staining of cell nuclei (original magnification ×400).

VZV gB Peptides Self-Aggregate Into Amyloid Fibrils and Accelerate Amylin and Aβ42 Aggregation

Synthesized viral peptides were tested for their ability to form amyloid using Thio-T. As ROI concentrations increased from 3 μM to 15 μM to 30 μM, ROIs 1 and 2 showed significant fold increases in fluorescence intensity compared to their lowest concentrations, indicating that these peptides self-aggregated to form amyloid (Figure 6A). In contrast, ROI 3 and the NEG peptide did not have increased fluorescence, indicating that they did not self-aggregate and form amyloid (Figure 6A). At the highest peptide concentration (30 μM), ROI 1 produced abundant amyloid fibrils on TEM, whereas NEG had no detectable fibrils (Figure 6B), confirming that fluorescence intensities were measuring amyloid.

To test whether VZV gB peptides accelerated amyloid formation in the presence of amylin, different concentrations (3 μM, 15 μM, or 30 μM) of ROI 1–3 and of the NEG peptide were incubated with 50 μM amylin for 24 hours then assayed by Thio-T. Compared to amylin alone, ROI 1 dose-dependently increased amyloid formation when added to amylin (Figure 6C). ROI 2 did not significantly increase amyloid formation in the presence of amylin. Interestingly, although ROI 3 did not self-aggregate, it significantly increased amyloid formation in the presence of amylin (Figure 6C). NEG peptide did not influence amyloid aggregation in the presence of amylin (Figure 6C). Similarly, different concentrations of each ROI 1–3 and NEG peptide (3 μM, 15 μM, or 30 μM) were incubated with 4 μM Aβ42 for 1 hour. Compared to Aβ42 alone, both ROI 1 (3, 15, and 30 μM) and ROI 3 (15 and 30 μM) peptides had significant fold increases in fluorescence (Figure 6D). Similar to amylin, the ROI 2 and NEG peptide did not accelerate Aβ42 aggregation (Figure 6D). Given the ability of ROI 3 to act as a catalyst, 15 μM of ROI 3 was incubated with a low (5 μM) or high (50 μM) concentration of amylin. Compared to 5 μM amylin alone, the addition of 15 μM of ROI 3 significantly reduced fluorescence, indicative of decreased amyloid (Figure 7). In contrast, compared to 50 μM amylin alone, the addition of 15 μM of ROI 3 significantly increased fluorescence, indicative of increased amyloid (Figure 7).

Together, these results indicate that specific VZV gB peptides can self-assemble to form amyloid and can accelerate amyloid fibrillization when exposed to an amyloidogenic cellular peptide. In addition, it appears that the decrease or increase in amyloid formation with ROI 3 is dependent on amylin concentrations.

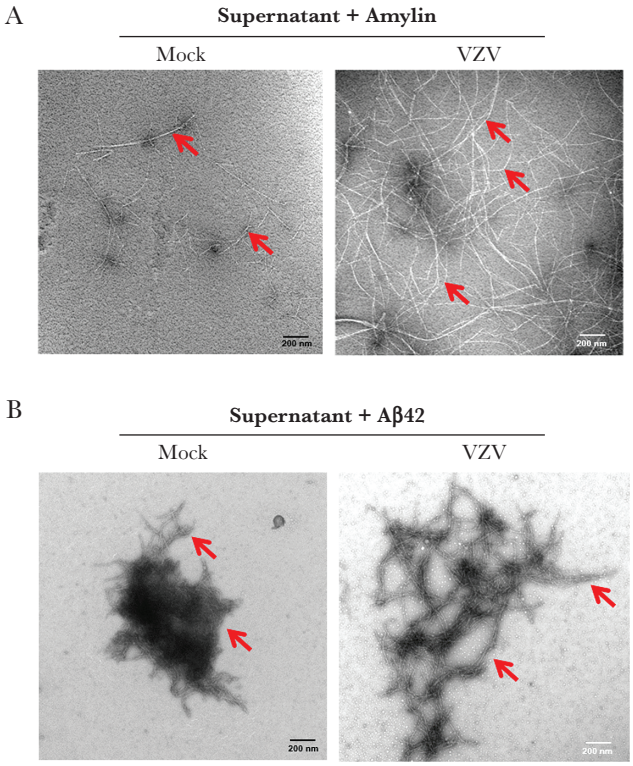

Figure 4. Varicella-zoster virus (VZV)-infected quiescent primary human spinal astrocytes (qHA-sps) produce an amyloidogenic extracellular environment. *A*, When incubated with 50 μM amylin for 72 hours, conditioned supernatant from mock-infected qHA-sps showed rare amyloid fibrils (red arrows), whereas supernatant from VZV-infected qHA-sps produced abundant amyloid fibrils (red arrows), as visualized by transmission electron microscopy. *B*, When incubated with 4 μM amyloid-β42 (Aβ42) for 1 hour, supernatant from mock-infected qHA-sps showed condensed amyloid fibrils, whereas supernatant from VZV-infected qHA-sps produced slightly more branched and elongated amyloid fibrils.

DISCUSSION

The spectrum of disease produced by protein misfolding and aggregation into toxic, proinflammatory amyloid species continues to expand with clinical disease corresponding to sites of aggregation, such as the brain, retina, and pancreas in AD, AMD, and DM, respectively. Triggers for amyloid formation are multifactorial and complex, involving interactions between environmental and host factors (genetic variants and age-associated changes such as decreased glymphatic clearance, altered extracellular matrix proteins, and immunosenescence); however, infectious agents have been proposed as triggers [16–18]. Elucidating the role of infection in amyloid disease progression is essential as pathogens may serve as early therapeutic targets.

Epidemiological reports show that VZV reactivation (zoster) increases dementia and neovascular AMD risk and decreases glycemic control in DM patients [6–9, 19]. Herein, we extended these association studies by demonstrating that direct VZV infection of qHA-sps increased expression of amyloidogenic proteins, amylin and APP/Aβ, and produced intracellular amyloid. These effects still occurred with acyclovir treatment indicating that cells already infected with VZV will continue to accumulate amyloidogenic peptides and amyloid within 3 DPI. However, in vivo and in the presence of immune cells/degrading enzymes, the persistence of VZV gB and continued amyloid accumulation may vary. VZV infection also resulted in an extracellular environment that promoted cellular peptide aggregation into amyloid fibrils that may be due, in part, to VZV gB peptides. These findings suggest that in combination with host and environmental factors, as well as virus-induced inflammation and cell death, VZV infection may accelerate toxic amyloid formation, contributing to amyloid-associated disease progression.

To our knowledge, VZV induction of amylin expression is the first demonstration of a virus regulating human amylin expression and provides a potential link between VZV infection, DM, and cognitive impairment. Amylin, a 37-residue peptide hormone that is expressed in pancreatic β cells, is cosecreted with insulin in the same vesicle and plays a role in glycemic regulation. In obese and insulin-resistant individuals, elevated circulating amylin levels (hyperamylinemia) are seen. Increased amylin concentrations lead to misfolding and oligomer/fibril formation in pancreatic islets, which deplete β cells and contribute to DM. Hyperamylinemia has also been associated with cognitive decline [20] with amylin and/or Aβ aggregates detected in AD brains [21, 22]. Aside from pancreatic β cells, amylin gene expression has been detected in neuroendocrine cells of the stomach, dorsal root ganglion [23–25], and developing kidney [26], although its function in these different cell types is not well characterized. The ability of VZV infection to induce intracellular amylin expression in astrocytes raises the intriguing possibility that during virus infection/reactivation, multiple cell types can be infected and induced to produce amylin. Depending on the ability of the infected cells to package and secrete amylin, hyperamylinemia may develop or worsen—leading to increased amyloid deposition. The spectrum of VZV-infected cells that produce and secrete amylin that can serve as a "seed" for amyloid formation remains to be determined. However, it is well established that VZV can infect neurons and glia, retina and associated vasculature, and pancreas in the context of AD, AMD, and DM, respectively, supporting the biological plausibility that infection at specific sites can contribute to different types of amyloid-associated diseases.

Determining how VZV induces amylin expression and amylin's function during viral infection provides potentially promising new avenues for future investigation. Specific amylin-inducing factors include monocyte chemoattractant protein-1 [27], tumor necrosis factor-α [28], and fatty acids [29]. Among these, fatty acids are likely candidates because VZV can increase fatty acid synthesis during infection [30], contributing to VZV glycoprotein maturation and to the synthesis of complete infectious virions [31]. The function of amylin during VZV infection still needs to be investigated. Amylin production may

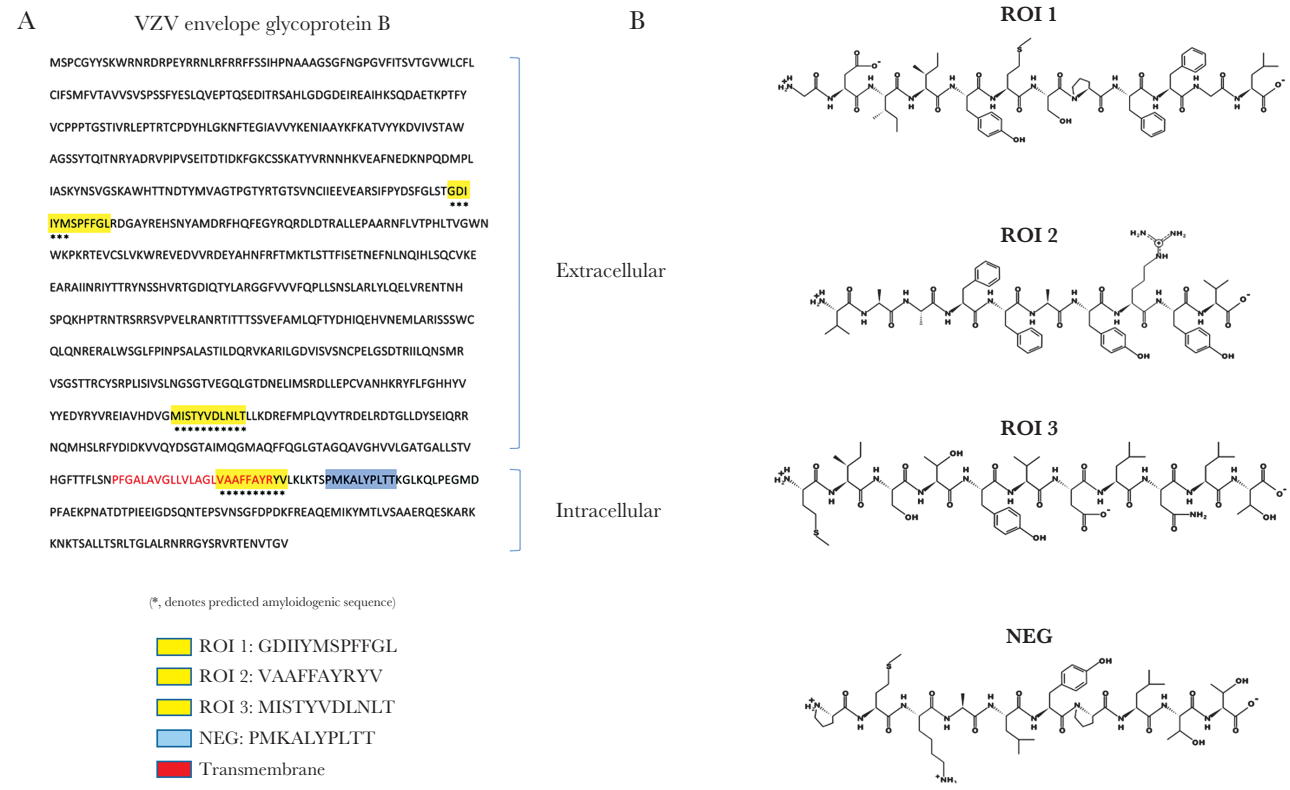

Figure 5. Varicella-zoster virus (VZV) glycoprotein B (gB) protein contains amyloidogenic sequences. *A*, Using the Waltz algorithm, 5 regions of VZV gB were predicted to be amyloidogenic; 3 peptides were selected spanning these amyloidogenic regions (*) and synthesized for further investigation (regions of interest [ROI] 1, 2, and 3; yellow). In addition, a peptide spanning a nonamyloidogenic region in VZV gB was synthesized (NEG; blue). *B*, Peptide structures are shown for ROI 1, ROI 2, and ROI 3, and NEG.

be antimicrobial—either through the formation of voltage-dependent, relatively nonselective ion channels in the cell membrane that kill the cell [32] or through amyloid formation that entraps the virus [17]. Alternatively, amylin/amyloid may play a different role, as demonstrated by functional amyloids found from bacteria to mammals that form biofilms and scaffolds, regulate melanin synthesis, and epigenetically control polyamines and information transfer (reviewed in reference [33]).

While VZV infection did not alter APP transcripts, APP protein was detected in VZV-infected cells but not mock-infected cells. This is consistent with a previous study showing that astrocytes contain APP transcripts but no protein due to a translation block; activation by interleukin IL-1α (IL-1α) or IL-1β releases this block and APP protein is produced [34]. In our case, VZV infection did not activate astrocytes, as demonstrated by the lack of infection-induced cytokine production [35]. Instead, VZV induced alterations within infected cells, but not uninfected bystander cells, and most likely released the APP translational block, leading to APP protein and/or Aβ peptide production. Thus, VZV-induced upregulation of 2 amyloidogenic cellular proteins (amylin and APP/Aβ) most likely promotes the formation of intracellular amyloid. It is important to note that in diseases associated with extracellular amyloid deposits, including AD, it has been proposed that the deposits originate intracellularly (reviewed in reference [36]), raising the possibility that following infection and subsequent virus-induced apoptosis, intracellular amyloid is released extracellularly, serving as a "seed" for further aggregation extracellularly.

Our finding that VZV-infected cell supernatant induced amyloidogenic peptide aggregation and formed amyloid fibrils, independent of secreted amylin or Aβ peptides, support the notion that VZV infection produces an amyloidogenic environment by stimulating the production of amyloid-promoting factors, by decreasing the activities of amyloid-inhibiting factors, or by both. Such factors have been reported, including (1) antichymotrypsin and apolipoprotein E that serve as pathological chaperones/amyloid catalysts binding to Aβ peptides and facilitating polymerization into amyloid filaments [37, 38], and (2) matrix metalloproteinase-9 that degrades amyloid fibrils [39].

Finally, aside from cellular amyloid-promoting factors, amyloidogenic peptides from pathogens have been described. Notably, peptides derived from human immunodeficiency virus-1 gp120 coreceptor binding region formed fibrils that enhanced infectivity in vitro [40] and an internal fragment of herpes simplex virus-1 gB, homologous to the carboxyl-terminal region of Aβ42, self-assembles into fibrils and accelerates Aβ42 fibrillization in primary rat cortical neurons in vitro [41]. We expanded upon

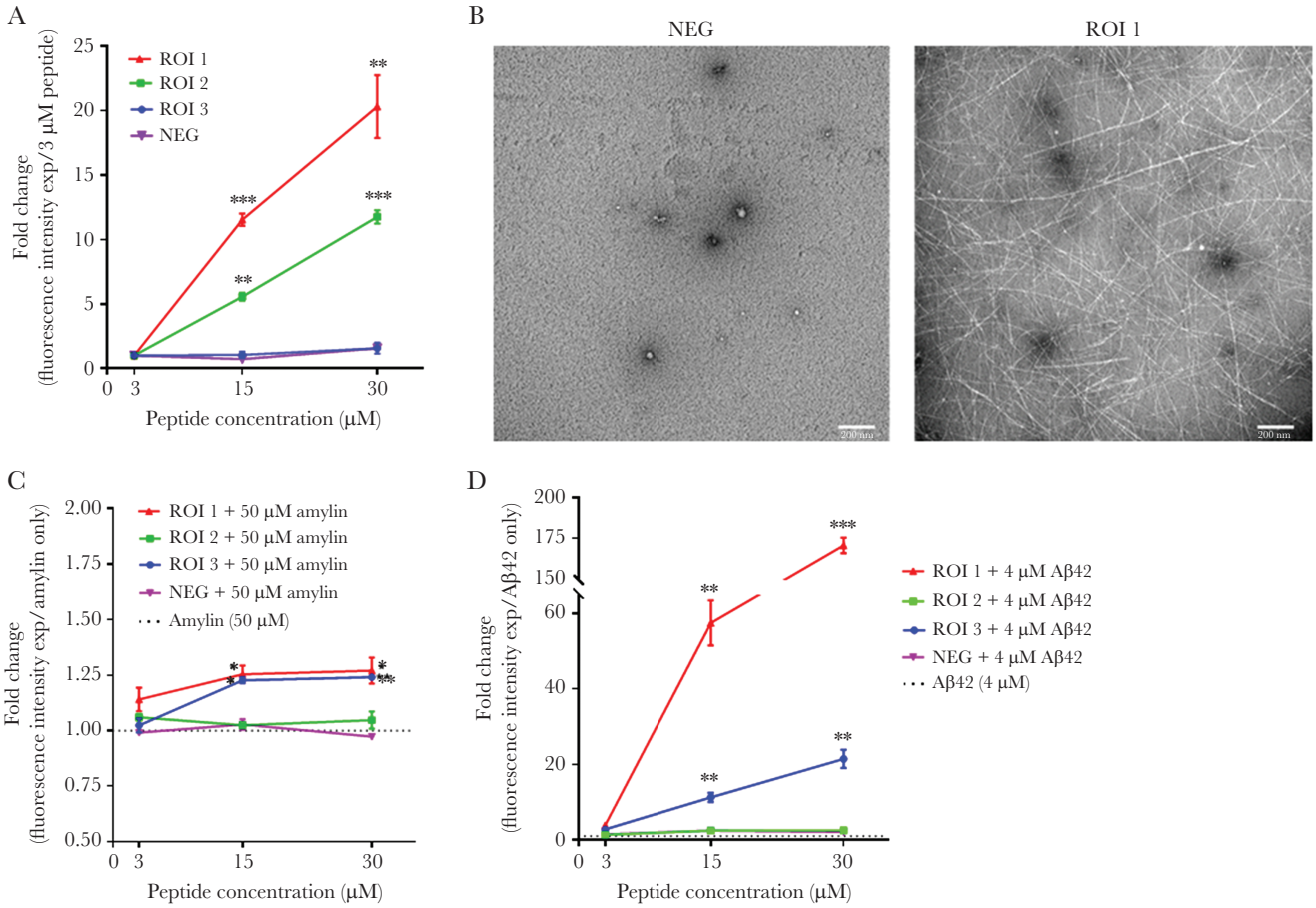

Figure 6. Peptides from varicella-zoster virus (VZV) glycoprotein B (gB) self-aggregate into amyloid fibrils and accelerate amylin and amyloid-β42 (Aβ42) aggregation. *A,* The regions of interest (ROI) 1 and ROI 2 peptides showed significant concentration-dependent increases in thioflavin-T (Thio-T) fluorescence at 15 and 30 μM relative to their 3 μM concentration, indicative of increasing amounts of amyloid. In contrast, the ROI 3 and nonamyloidogenic (NEG) peptides did not show changes in Thio-T fluorescence with increasing concentrations. **P* < .05, ***P* < .01, ****P* < .001; n = 3 independent experiments. *B,* Transmission electron microscopy showed no amyloid fibrils at the highest concentration of the NEG peptide (30 μM) but abundant amyloid fibrils at the highest concentration of ROI 1 (30 μM), corroborating the Thio-T assay and indicating that ROI 1 can self-aggregate to form amyloid fibrils. *C,* When combined with 50 μM amylin, ROI 1 and ROI 3 peptides (15 and 30 μM) showed significant fold increases in Thio-T fluorescence compared to 50 μM amylin alone. In contrast, ROI 2 and NEG peptides did not show differences in Thio-T fluorescence at increasing concentrations compared to 50 μM amylin alone. The dotted line shows Thio-T fluorescence for 50 μM amylin only. **P* < .05, ***P* < .01; n = 3 independent experiments. *D,* When combined with 4 μM Aβ42, ROI 1 and ROI 3 (15 and 30 μM) showed significant fold increases in Thio-T fluorescence compared to 4 μM Aβ42 alone. In contrast, ROI 2 and NEG peptides showed no differences in Thio-T fluorescence at increasing concentrations compared to 4 μM Aβ42 alone. The dotted line shows Thio-T fluorescence for 4 μM Aβ42 only. ***P* < .01, ****P* < .001; n = 3 independent experiments.

these studies by identifying 3 unique regions of VZV gB that can self-assemble, accelerate Aβ42 and amylin fibrillization, or both. ROI 1 self-assembled and accelerated Aβ42 and amylin fibrillization. However, although ROI 2 self-assembled, it did not accelerate Aβ42 or amylin fibrillization. In contrast, ROI 3 failed to self-assemble, yet acted as a catalyst for Aβ42 and amylin fibrillization. A recent study revealed concentration-dependent effects of amylin on AD pathology [42]. Lower concentrations of amylin appeared to reverse Aβ-induced tau phosphorylation and neuronal damage but high concentrations accelerated these processes [42]. Similarly, we found concentration-dependent amylin effects on amyloid formation. When combined with a constant ROI 3 concentration, a low concentration of amylin reduced amyloid, whereas a high concentration of amylin increased amyloid, compared to amylin alone. The cleavage/degradation of VZV gB during infection to produce amyloidogenic/catalytic peptides and the physical characteristics mediating the unique properties of the VZV gB peptide fragments is an essential next step, but our findings suggest that during infection of cells with elevated levels of amyloidogenic cellular peptides from environmental or host factors (ie, amylin-producing pancreatic β cells), the viral peptides may accelerate amyloid formation.

VZV-induced intracellular deposition of amyloid and the ability of viral peptides to self-aggregate and form amyloid fibrils challenge the notion that a pathogen must be present in diseased tissue to be causative. We must now consider contributions of virus-induced intracellular amyloid and viral peptides to amyloidogenesis, because even after viral DNA and RNA

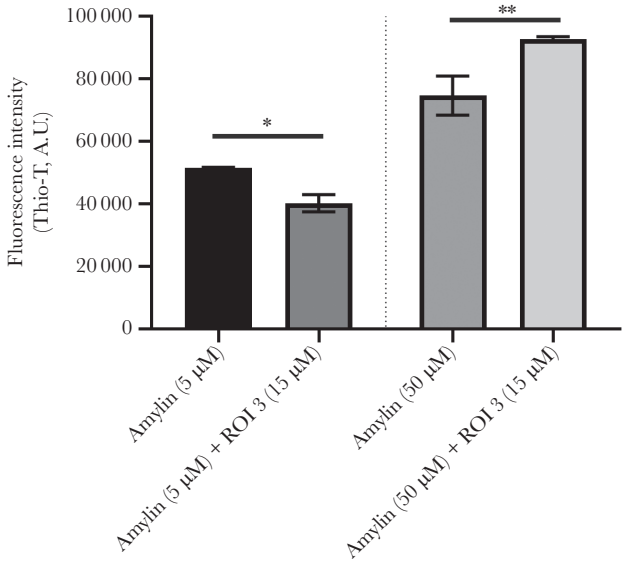

Figure 7. Amylin has dose-dependent effects on amyloid formation in the presence of region of interest (ROI) 3. A low (5 μM) and high (50 μM) concentration of amylin was combined with 15 μM ROI 3 and amyloid levels measured by a thioflavin-T (Thio-T) assay. Compared to amylin alone at 5 μM, amylin plus ROI 3 (15 μM) had significantly lower Thio-T fluorescence. In contrast, amylin at 50 μM plus ROI 3 (15 μM) had significantly higher Thio-T fluorescence compared to 50 μM amylin alone. $^{*}P < .05$, $^{**}P < .01$. Bars represent standard error of the mean.

have been cleared, both intracellular amyloid released extracellularly from infected cells and residual viral peptides can potentially serve as a nidus for amyloid formation, inflammation, and/or cytotoxicity. Because clinical disease can occur decades after the initial insult, our examination of diseased, amyloid-containing tissues may miss earlier contributions from pathogens. The identification of these pathogens and the underlying mechanisms by which they promote an amyloidogenic environment will provide early therapeutic targets that may potentially attenuate progression of amyloid-associated diseases.

Notes

Acknowledgments: We thank Heidi Chial for editorial review and Cathy Allen for manuscript preparation. Imaging experiments were performed in the University of Colorado Anschutz Medical Campus Advanced Light Microscopy Core.

Financial support. This work was supported by the National Institutes of Health (grant numbers PO1 AG032958 (National Institute on Aging) to M. A. N., R. M., and R. J. C., and R01 NS093716 (National Institute of Neurological Disorders and Stroke) to M. A. N., A. N. B., and R. J. C.); the Fisher Family Foundation (to H. P.); and the Rocky Mountain Neurological Disorders Core (grant number P30NS048154 to the University of Colorado Anschutz Medical Campus Advanced Light Microscopy Core).

Potential conflicts of interest. All authors: no reported conflicts. All authors have submitted the ICMJE Form for Disclosure of Potential Conflicts of Interest. Conflicts that the editors consider relevant to the content of the manuscript have been disclosed.

References

1. Kennedy PG, Grinfeld E, Gow JW. Latent varicella-zoster virus is located predominantly in neurons in human trigeminal ganglia. Proc Natl Acad Sci U S A **1998**; 95:4658–62.
2. Kennedy PG, Grinfeld E, Gow JW. Latent varicella-zoster virus in human dorsal root ganglia. Virology **1999**; 258:451–4.
3. Nagel MA, Rempel A, Huntington J, Kim F, Choe A, Gilden D. Frequency and abundance of alphaherpesvirus DNA in human thoracic sympathetic ganglia. J Virol **2014**; 88:8189–92.
4. Gilden D, Nagel MA, Cohrs RJ, Mahalingam R. The variegate neurological manifestations of varicella zoster virus infection. Curr Neurol Neurosci Rep **2013**; 13:374.
5. Gershon M, Gershon A. Varicella-zoster virus and the enteric nervous system. J Infect Dis **2018**; 218:113–9.
6. Tsai MC, Cheng WL, Sheu JJ, et al. Increased risk of dementia following herpes zoster ophthalmicus. PLoS One **2017**; 12:e0188490.
7. Chen VC, Wu SI, Huang KY, et al. Herpes zoster and dementia: a nationwide population-based cohort study. J Clin Psychiatry **2018**; 79:16m11312.
8. Ho JD, Lin HC, Kao LT. Increased risk of neovascular age-related macular degeneration in patients with herpes zoster ophthalmicus: a retrospective cohort study. Acta Ophthalmol **2019**; 97:e321–2.
9. Munoz-Quiles C, López-Lacort M, Ampudia-Blasco FJ, Diez-Domingo J. Risk and impact of herpes zoster on patients with diabetes: a population-based study, 2009–2014. Hum Vaccin Immunother **2017**; 13:2606–11.
10. de Silva SM, Mark AS, Gilden DH, et al. Zoster myelitis: improvement with antiviral therapy in two cases. Neurology **1996**; 47:929–31.
11. Bubak AN, Como CN, Blackmon AM, et al. Varicella zoster virus induces nuclear translocation of the neurokinin-1 receptor, promoting lamellipodia formation and viral spread in spinal astrocytes. J Infect Dis **2018**; 218:1324–35.
12. Cohrs RJ, Gilden DH. Prevalence and abundance of latently transcribed varicella-zoster virus genes in human ganglia. J Virol **2007**; 81:2950–6.
13. Mahalingam R, Wellish M, Cohrs R, et al. Expression of protein encoded by varicella-zoster virus open reading frame 63 in latently infected human ganglionic neurons. Proc Natl Acad Sci U S A **1996**; 93:2122–4.
14. Yonemoto IT, Kroon GJ, Dyson HJ, Balch WE, Kelly JW. Amylin proprotein processing generates progressively more amyloidogenic peptides that initially sample the helical state. Biochemistry **2008**; 47:9900–10.

15. Vafai A, Wroblewska Z, Mahalingam R, et al. Recognition of similar epitopes on varicella-zoster virus gpI and gpIV by monoclonal antibodies. J Virol **1988**; 62:2544–51.
16. Torrent M, Pulido D, Nogués MV, Boix E. Exploring new biological functions of amyloids: bacteria cell agglutination mediated by host protein aggregation. PLoS Pathog **2012**; 8:e1003005.
17. Eimer WA, Vijaya Kumar DK, Navalpur Shanmugam NK, et al. Alzheimer's disease-associated β-amyloid is rapidly seeded by herpesviridae to protect against brain infection. Neuron **2018**; 99:56–63.e3.
18. Readhead B, Haure-Mirande JV, Funk CC, et al. Multiscale analysis of independent Alzheimer's cohorts finds disruption of molecular, genetic, and clinical networks by human herpesvirus. Neuron **2018**; 99:64–82.e7.
19. Kawai K, Yawn BP. Risk factors for herpes zoster: a systematic review and meta-analysis. Mayo Clin Proc **2017**; 92:1806–21.
20. Ly H, Despa F. Hyperamylinemia as a risk factor for accelerated cognitive decline in diabetes. Expert Rev Proteomics **2015**; 12:575–7.
21. Jackson K, Barisone GA, Diaz E, Jin LW, DeCarli C, Despa F. Amylin deposition in the brain: a second amyloid in Alzheimer disease? Ann Neurol **2013**; 74:517–26.
22. Oskarsson ME, Paulsson JF, Schultz SW, Ingelsson M, Westermark P, Westermark GT. In vivo seeding and cross-seeding of localized amyloidosis: a molecular link between type 2 diabetes and Alzheimer disease. Am J Pathol **2015**; 185:834–46.
23. Gebre-Medhin S, Mulder H, Zhang Y, Sundler F, Betsholtz C. Reduced nociceptive behavior in islet amyloid polypeptide (amylin) knockout mice. Brain Res Mol Brain Res **1998**; 63:180–3.
24. Tingstedt JE, Edlund H, Madsen OD, Larsson LI. Gastric amylin expression. Cellular identity and lack of requirement for the homeobox protein PDX-1. A study in normal and PDX-1-deficient animals with a cautionary note on antiserum evaluation. J Histochem Cytochem **1999**; 47:973–80.
25. Zaki M, Koduru S, McCuen R, Vuyyuru L, Schubert ML. Amylin, released from the gastric fundus, stimulates somatostatin and thus inhibits histamine and acid secretion in mice. Gastroenterology **2002**; 123:247–55.
26. Wookey PJ, Tikellis C, Nobes M, Casley D, Cooper ME, Darby IA. Amylin as a growth factor during fetal and postnatal development of the rat kidney. Kidney Int **1998**; 53:25–30.
27. Cai K, Qi D, Hou X, et al. MCP-1 upregulates amylin expression in murine pancreatic β cells through ERK/JNK-AP1 and NF-κB related signaling pathways independent of CCR2. PLoS One **2011**; 6:e19559.
28. Cai K, Qi D, Wang O, et al. TNF-α acutely upregulates amylin expression in murine pancreatic beta cells. Diabetologia **2011**; 54:617–26.
29. Qi D, Cai K, Wang O, et al. Fatty acids induce amylin expression and secretion by pancreatic beta-cells. Am J Physiol Endocrinol Metab **2010**; 298:E99–E107.
30. Jerkofsky M, De Siervo AJ. Differentiation of strains of varicella-zoster virus by changes in neutral lipid metabolism in infected cells. J Virol **1986**; 57:809–15.
31. Namazue J, Kato T, Okuno T, Shiraki K, Yamanishi K. Evidence for attachment of fatty acid to varicella-zoster virus glycoproteins and effect of cerulenin on the maturation of varicella-zoster virus glycoproteins. Intervirology **1989**; 30:268–77.
32. Mirzabekov TA, Lin MC, Kagan BL. Pore formation by the cytotoxic islet amyloid peptide amylin. J Biol Chem **1996**; 271:1988–92.
33. Maury CP. The emerging concept of functional amyloid. J Intern Med **2009**; 265:329–34.
34. Rogers JT, Leiter LM, McPhee J, et al. Translation of the Alzheimer amyloid precursor protein mRNA is up-regulated by interleukin-1 through 5'-untranslated region sequences. J Biol Chem **1999**; 274:6421–31.
35. Bubak AN, Como CN, Blackmon AM, Jones D, Nagel MA. Varicella zoster virus differentially alters morphology and suppresses proinflammatory cytokines in primary human spinal cord and hippocampal astrocytes. J Neuroinflammation **2018**; 15:318.
36. LaFerla FM, Green KN, Oddo S. Intracellular amyloid-beta in Alzheimer's disease. Nat Rev Neurosci **2007**; 8:499–509.
37. Ma J, Yee A, Brewer HB Jr, Das S, Potter H. Amyloid-associated proteins alpha 1-antichymotrypsin and apolipoprotein E promote assembly of Alzheimer beta-protein into filaments. Nature **1994**; 372:92–4.
38. Potter H, Wisniewski T. Apolipoprotein e: essential catalyst of the Alzheimer amyloid cascade. Int J Alzheimers Dis **2012**; 2012:489428.
39. Yan P, Hu X, Song H, et al. Matrix metalloproteinase-9 degrades amyloid-beta fibrils in vitro and compact plaques in situ. J Biol Chem **2006**; 281:24566–74.
40. Tan S, Li L, Lu L, et al. Peptides derived from HIV-1 gp120 co-receptor binding domain form amyloid fibrils and enhance HIV-1 infection. FEBS Lett **2014**; 588:1515–22.
41. Cribbs DH, Azizeh BY, Cotman CW, LaFerla FM. Fibril formation and neurotoxicity by a herpes simplex virus glycoprotein B fragment with homology to the Alzheimer's A beta peptide. Biochemistry **2000**; 39:5988–94.
42. Gan Q, Yao H, Na H, et al. Effects of amylin against amyloid-β-induced tauopathy and synapse loss in primary neurons. J Alzheimers Dis **2019**; 70:1025–40.